Chalcogenide Letters

Tech Science Press

http://doi.org/10.32604/cl.2026.082805

REVIEW

Review of the Application of Tellurium and Tellurides in Sodium Metal Batteries

Shan Yuan[1,2], Fei Wang[2,*], Jinping Zhang[2,*], Yuxin Jiang[2], Kaibo Gu[2], Chenhao Qiao[2], Yutong Bai[2], Jie Yu[2], Quan Chen[1] and Dedi Han[3]

[1]School of Materials Science and Engineering, Henan University of Science and Technology, Luoyang, China
[2]Faculty of Engineering, Huanghe Science and Technology College, Zhengzhou, China
[3]Henan Zhongfu Industrial Co., Ltd., Gongyi, China
*Corresponding Authors: Fei Wang. Email: wangf157@hhstu.edu.cn; Jinping Zhang. Email: jpzhang@hhstu.edu.cn

Received: 23 March 2026; Accepted: 20 April 2026; Published: 09 May 2026

ABSTRACT: Sodium metal batteries stand as a highly promising electrochemical energy storage system; however, their commercialization is severely impeded by challenges such as anode dendrite formation, the shuttle effect of highly reactive intermediates at the cathode, electrode volume expansion, and interfacial instability. Owing to their high electronic conductivity, high theoretical specific capacity, and superior sodiumphilic affinity, tellurium and its tellurides have emerged as pivotal functional materials for enhancing the performance of sodium metal batteries. This study reviews the advancements in their applications within sodium metal batteries, elaborates rational design strategies carbon-based composites, alloying, and heterostructure construction for cathode functional materials, analyzes their mechanisms in optimizing sodium ion migration kinetics and synergistically regulating the solid electrolyte interphase (SEI) layer at the anode interface, and summarizes full-cell performance optimization strategies such as eutectic acceleration, defect engineering, and multicomponent synergy regulation. Additionally, it critically analyzed such as the scarcity of tellurium resources, inadequate long-term cycling stability of materials, and ambiguous reaction mechanisms. Furthermore, it outlines future research directions in terms of resource utilization, mechanism investigation, structural design, and process optimization, providing significant guidance for research and development in this field.

KEYWORDS: Tellurium and telluride; sodium metal battery; cathode material; anode interface regulation; performance optimization; electrochemical energy storage

1 Introduction

1.1 Research Background and Significance

Against the backdrop of the transition of the global energy structure towards clean and low-carbon sources, electrochemical energy storage technology has emerged as a cornerstone for new energy integration and smart grid development [1]. Consequently, improving its performance and promoting industrial upgrading have become pivotal focuses [2]. Traditional lithium-ion batteries, with their well-established technological system, currently dominate the energy storage market [3]. Nevertheless, their reliance on lithium resources, which are characterized by limited reserves, uneven geographical distribution, and price volatility [3], poses significant challenges to meeting the escalating demand for cost-effective, high-capacity energy storage solutions in sectors such as large-scale energy storage systems and low-speed

electric vehicles [4]. Consequently, the exploration of novel alkali metal ion battery systems has garnered considerable attention within the energy storage research community [5]. The aforementioned advantages, owing to its electrochemical properties similar to those of lithium, abundant natural reserves, and low extraction costs, has positioned sodium-based electrochemical energy storage systems as a highly promising alternative to lithium-ion batteries [6]. Notably, sodium metal batteries, boasting a high theoretical specific capacity of 1166 $mAh{\cdot}g^{-1}$ and a low reduction potential of −2.71 V (versus standard hydrogen electrode (SHE)) [7], as the preferred choice for high-energy-density energy storage devices, with broad application prospects in large-scale electrochemical energy storage and portable electronic devices [8]. Telluride-based nanomaterials have exhibited remarkable potential as advanced electrodes for supercapacitors owing to their excellent electrical conductivity, unique structural features, and impressive electrochemical properties [9]. Copper telluride nanoparticles, nickel cobalt telluride nanotubes, and cobalt telluride nanorods, synthesized via facile hydrothermal or solvothermal methods, have been successfully employed as high-performance supercapacitor electrodes [10]. These nanostructured tellurides deliver large specific capacitance/capacity, outstanding rate capability, and long cyclic stability up to 10,000 cycles. In particular, bimetallic tellurides with rational nanotubular or interpenetrating network structures can provide efficient ion and electron transport pathways, significantly boosting energy and power densities [11]. Compared with conventional metal sulfides and selenides, metal tellurides show superior electronic conductivity and pseudocapacitive behavior, making them promising electrode candidates for supercapacitors [12]. The successful design and optimization of telluride-based electrodes in supercapacitors, including nanostructure engineering, morphology control, and carbon/composite integration, offer valuable strategies for enhancing the structural stability, ion diffusion kinetics, and charge transfer efficiency of tellurium-based electrodes in sodium metal batteries.

1.2 Research Status

The commercialization of sodium metal batteries is hindered by several critical challenges that require urgent addressing, presenting more formidable obstacles than those encountered in lithium-ion batteries [13]. During the charge-discharge cycles, the sodium metal anode is susceptible to random dendritic growth (Fig. 1). The growth protrusion of these dendrites can puncture the battery separator, leading to internal short circuits and posing significant safety risks [14,15]. Furthermore, dendrite formation exacerbates side reactions at the electrode surface, causing a decrease in battery Coulombic efficiency (CE) [16]. Concurrently, cathode materials suffer from low electrical conductivity and sluggish electrochemical reaction kinetics [17]. Mainstream cathode materials, such as sulfur- [18] and selenium-based [19] compounds, generate soluble intermediates like polysulfides and polyselenides during electrochemical reactions. These intermediates easily diffuse in the electrolyte, causing active material loss and rapid battery capacity degradation [20]. Additionally, severe volume expansion of electrodes during sodium insertion/extraction processes further compromises electrode structural integrity and reduces battery cycling stability [21]. Moreover, the poor interfacial compatibility between the electrodes and the electrolyte in sodium metal batteries often results in the formation of an unstable solid electrolyte interphase (SEI) layer [22]. This layer experience repeated cracking and reformation during cycling, which continuously consumes the electrolyte and active Na metal, thereby elevating the interfacial impedance of the battery and significantly degrading overall electrochemical performance [23]. These issues are interrelated and mutually reinforcing, essentially stemming from the intrinsic correlation between thermodynamic instability and kinetic limitations within the battery system [24]. Single-factor modulation strategies are insufficient to fundamentally resolve this

core contradiction, which constitutes a major bottleneck for the practical application of sodium metal batteries [25].

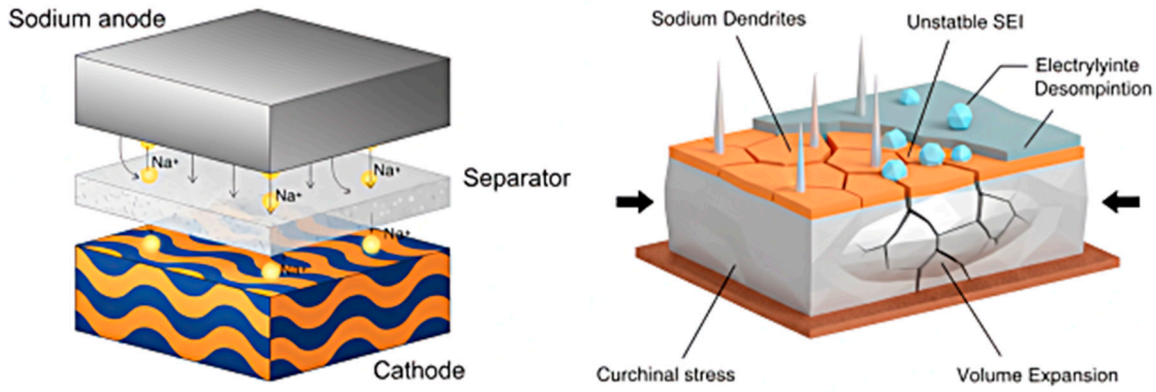

Figure 1: The structure and common issues of sodium-metal batteries.

To surmount these technical hurdles, researchers have turned their attention to chalcogen element modification strategies [26]. Incorporating chalcogen elements (e.g., S, Se, Te) to modify and optimize the positive and negative electrodes and interfaces of sodium metal batteries, the aim is to achieve comprehensive performance enhancements [27,28]. Among these chalcogens, tellurium has emerged as the research focus for the modification of SMBs, owing to its exceptional physicochemical and electrochemical properties [29,30]. Compared to sulfur and selenium, tellurium exhibits superior electronic conductivity (up to 5 $S{\cdot}cm^{-1}$), which is much higher than that of S [30] (5×10^{-30} $S{\cdot}cm^{-1}$) and Se [31] (1×10^{-3} $S{\cdot}cm^{-1}$), thereby effectively addressing electrode conductivity issues [32]. Additionally, tellurium possesses a high theoretical specific capacity (420 $mAh{\cdot}g^{-1}$) and density (6.2 $g{\cdot}cm^{-3}$), endowing it with inherent advantages for improving battery energy density [33]. Crucially, tellurium and its compounds can not only mitigate the core challenges associated with cathode materials by suppressing the shuttle effect of polysulfides and polytellurides, alleviating volume expansion, and accelerating electrochemical reaction kinetics through physical confinement, chemical adsorption, and catalytic conversion but also act on the sodium metal anode by constructing artificial SEI layers, optimizing sodium deposition behavior, and inhibiting dendrite growth [32]. This dual-action approach enhances the cycling stability and safety of the anode while simultaneously optimizing the performance of both electrodes in sodium metal batteries.

However, among chalcogen-based materials, tellurium and tellurides still present unique and irreplaceable merits that justify continued research priority despite their resource scarcity and relatively higher cost, compared with sulfides, selenides, oxides, and conventional transition metal compounds. First, tellurium has an exceptional electronic conductivity up to 5 $S{\cdot}cm^{-1}$, which is nearly 10^{30} times higher than sulfur and five orders of magnitude higher than selenium [34], fundamentally overcoming the poor electron-transport limitation that plagues most sulfur and selenium cathodes. Second, tellurides show strong sodium-philicity and low Na^+ diffusion energy barriers, effectively regulating Na deposition behavior and suppressing dendrite growth, which is difficult to achieve with sulfides and selenides under the same conditions. Third, tellurides can induce the formation of dense, inorganic-rich SEI layers with high mechanical strength and interfacial stability, remarkably reducing electrolyte decomposition and side reactions [35]. Fourth, Te-based materials exhibit good compatibility with carbonate-based electrolytes [36], whereas traditional sulfur cathodes often require ether electrolytes with high flammability, thus expanding

the safe application scenarios of sodium metal batteries. Therefore, even with resource constraints, tellurium and tellurides remain indispensable for addressing the critical bottlenecks of SMBs and cannot be simply replaced by low-cost sulfides, selenides or oxides.

1.3 Objective and Scope of the Review

In recent years, great progress has been made in the research on the application of tellurium and its compounds in sodium metal batteries [37]. As core functional materials, they have been widely used as cathode active materials, anode interface protectants, and battery performance modulators, with related modification strategies and technical routes being continuously optimized and upgraded. Although several reviews have summarized telluriu-based materials for rechargeable batteries, most focus on Li-Te systems or single-electrode optimization. This review systematically summarizes the dual roles of tellurium and telluride in "cathode modification and anode interface control" of sodium metal batteries. The clear relationship between the structure and performance of Telluride design and the electrochemical performance of the whole battery is established, which provides a unique guidance for reasonable material design.

2 Tellurium and Tellurides as Core Functional Materials for Cathodes

As the core component for battery energy storage and conversion, cathode materials directly dictate the overall performance of batteries. Tellurium (Te) and its tellurides, boasting intrinsic advantages such as exceptionally high electronic conductivity (Te: 5 $S{\cdot}cm^{-1}$, significantly surpassing sulfur's 5×10^{-30} $S{\cdot}cm^{-1}$ and selenium's 1×10^{-3} $S{\cdot}cm^{-1}$), high theoretical specific capacity (420 $mAh{\cdot}g^{-1}$), and high density (6.2 $g{\cdot}cm^{-3}$), effectively mitigate the challenges traditional sulfur-based cathodes, including poor conductivity, severe volume expansion, and the polysulfide shuttle effect (Table 1).

Table 1: Comparison of key electrochemical performance of tellurium based cathode in sodium battery.

System Type	Cathode Material	Initial Discharge Capacity ($mAh{\cdot}g^{-1}$)	Cycling	Rate	Citation
Na-Te Battery	CeO_2-QDs/HPC@Te	625.5	0.5 C, 200 cycles; 364.4 $mAh{\cdot}g^{-1}$; 98%	20 C/190 $mAh{\cdot}g^{-1}$	[38]
Na-Te Battery	Porous Carbon Nanorods@Te	402	0.2 C, 500 cycles; 348 $mAh{\cdot}g^{-1}$; 86.7%	8 C/122 $mAh{\cdot}g^{-1}$	[39]
Na-Te Battery	CMK-3@Te	367	0.2 C, 500 cycles; 310 $mAh{\cdot}g^{-1}$	2 C/230 $mAh{\cdot}g^{-1}$	[40]
Na-Te-S Battery	$Te_{0.1}S_{0.9}$/CMK-3	1250	0.25 $A{\cdot}g^{-1}$, 100 cycles; 845 $mAh{\cdot}g^{-1}$	5 $A{\cdot}g^{-1}$/590 $mAh{\cdot}g^{-1}$	[41]
Na-S Battery	3D Flower-like $MoTe_2$@S	1015	0.1 C, 300 cycles; 1004 $mAh{\cdot}g^{-1}$; 99%	2 C/414 $mAh{\cdot}g^{-1}$	[42]
Na-S Battery	Janus MoSTe@S (DFT)	—	—	Reduced energy barriers, suppressed shuttle	[43]
Na-Te Battery	N-doped porous carbon sponge@Te (NPCS/Te)	628	0.5 C, 100 cycles; 303 $mAh{\cdot}g^{-1}$	10 C/252 $mAh{\cdot}g^{-1}$	[44]

2.1 Composite with Carbon-Based Materials

Carbon materials, due to their high electronic conductivity, hierarchical porous structure, and excellent structural stability, have become ideal composite carriers for tellurium and tellurides. They inhibit the shuttling and volume expansion of polytellurides (Na_nTe_m) through physical confinement effects, while enhancing electron transport efficiency [40].

Koketsu et al. [40] adopted a melt impregnation method (Fig. 2a) to infiltrate Te into ordered mesoporous carbon CMK-3, preparing Te@CMK-3 composites. The mesoporous structure of CMK-3 enabled the uniform dispersion of Te, and its specific surface area decreased from 1231 $m^2 \cdot g^{-1}$ to 70 $m^2 \cdot g^{-1}$, confirming that Te was successfully filled into the mesoporous channels (Fig. 2b) [40]. This composite material exhibits superior electrochemical performance in carbonate-based electrolytes, maintaining 55% of the theoretical capacity at 2 C; its coulombic efficiency remains nearly 100% after 500 cycles, the coulombic efficiency remains close to 100% (Fig. 2c). Li et al. [44] designed nitrogen-doped hierarchical porous carbon sponges (NPCS) as Te hosts, via a sacrificial template method to construct a hierarchical micro/meso/macroporous structure, where mesopores serve for Te loading (Fig. 2d), macropores alleviate volume expansion, and nitrogen doping further enhances electronic conductivity and strengthens the adsorption capacity for polyselenides (Fig. 2e). The NPCS/Te composite cathode delivers a specific capacity of 252 $mAh \cdot g^{-1}$ at a high rate of 10 C, demonstrating excellent rate performance [44]. Wang et al. [39] prepared porous carbon nanorods (C_p) via KOH activation and combined them with Te to form a Te/C_p cathode (Fig. 2f). The conductive network of the carbon nanorods accelerates electron transport, and the porous structure inhibits the dissolution of polyselenides. In a 2.5 M ether-based electrolyte, the specific capacity reaches 399 $mAh \cdot g^{-1}$ at 0.2 C, and after 1000 cycles at 8 C, retains a specific capacity of 126 $mAh \cdot g^{-1}$ (Fig. 2g).

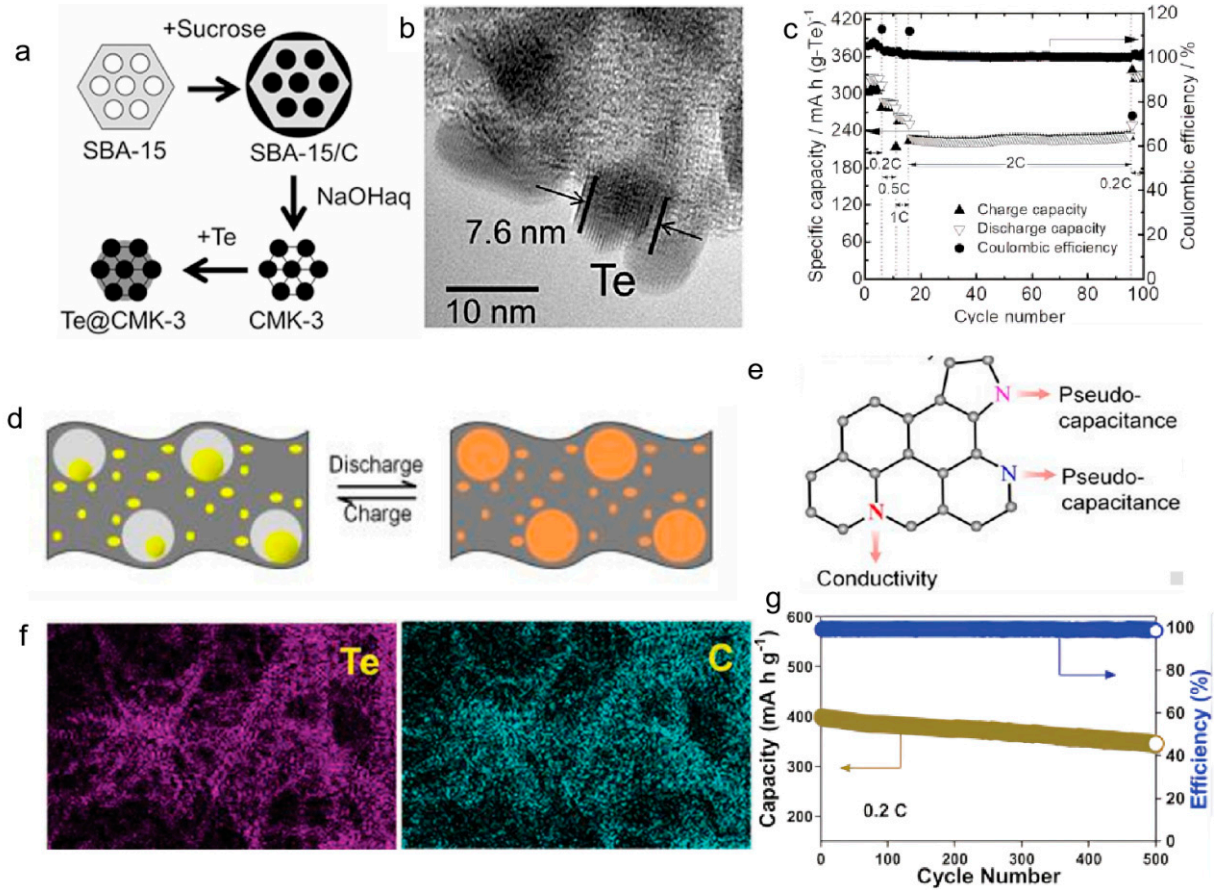

Figure 2: (**a**) A synthetic route of the Te@CMK-3 composite [40]; (**b**) its high-magnification images [40]; (**c**) cycling proper ties at 0.2 C, 0.5 C, 1 C, and 2 C [40]; (**d**) Structural characteristics of NPCS/Te composite materials [44]; (**e**) schematic illustration of N atoms in Na-Te batteries [44]; (**f**) elemental mapping results of the Te/Cp composite [39]; (**g**) Cyclability of the Na metal-Te cells with a 2.5 m electrolyte at 0.2 C [39].

2.2 Alloying of Tellurium-Based Compounds

By forming alloy compounds with chalcogen elements such as sulfur and selenium through Te (e.g., Te_xS_{1-x}), or forming tellurides with transition metals (e.g., $MoTe_2$), intramolecular chemical interactions enhance the adsorption of electrochemical reactive intermediates, while modulating electrochemical kinetics.

Sun et al. [41] adopted a melt infiltration method to uniformly confines heteroatomic Te_xS_{1-x} species within CMK-3 mesopores (Fig. 3a). The high polarity of Te-S bonds not only enhances the intrinsic conductivity of the material (higher than that of pure S_8 molecules) but also induce the formation of a solid electrolyte interphase (SEI) layer (Fig. 3b), effectively preventing side reactions between polysulfides/polytellurides and the carbonate electrolyte. Among these, the $Te_{0.1}S_{0.9}$/CMK-3 composite retains a specific capacity of 485 $mAh{\cdot}g^{-1}$ and achieves a coulombic efficiency of 99.6% after undergoing 500 cycles at a current density of 1 $A{\cdot}g^{-1}$ (Fig. 3c). Gao et al. [42] designed a 3D flower-like molybdenum ditelluride ($MoTe_2$) to act as both a sulfur immobilizer and a catalyst (Fig. 3d). Its unique nanosheet assembly architecture provides abundant active sites (Fig. 3e). The polar surface of $MoTe_2$ effectively suppresses polysulfide shuttling via chemical adsorption, concurrently expediting the kinetics of redox reactions. The MoTe/S composite cathode exhibits a capacity retention of 498 mAh g^{-1} after 500 cycles at a 1 C rate, while the as-assembled pouch cell exhibits stable cycling for 40 cycles under practical conditions. Janus-type transition metal dichalcogenides [43] (e.g., MoSTe) (Fig. 2f) enhance the chemisorption of Na_2S_n by via of their out-of-plane asymmetric structural configuration (with a binding energy ranging from −1.18 to −2.48 eV, which is lower than that between the electrolyte and Na_2Sn) (Fig. 3g), while concurrently reducing the decomposition energy barrier of Na_2S and the diffusion energy barrier of Na^+, thereby significantly improving the charge transfer efficiency (Fig. 3h).

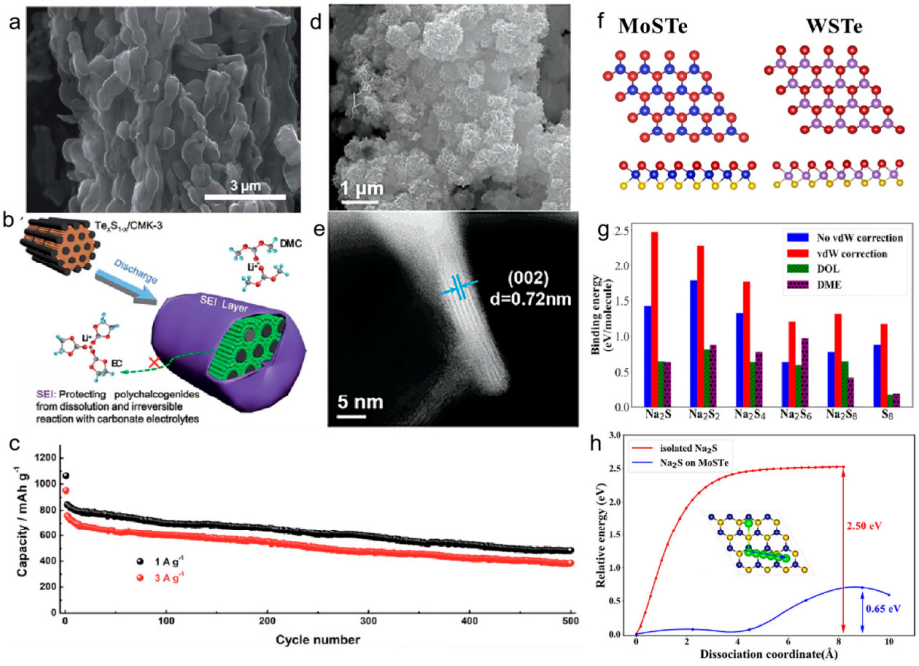

Figure 3: (**a**) SEM images of $Te_{0.1}S_{0.9}$/CMK-3 [41]; (**b**) Schematic diagram of the Te-induced formation of SEI layers on the Te_xS_{1-x}/CMK-3 electrode surfaces [41]; (**c**) Long-term cycling performance of Te_xS_{1-x}/CMK-3 at 1 and 3 $A{\cdot}g^{-1}$ [41]; (**d**,**e**) SEM images of the $MoTe_2$ under different magnifications [42]; (**f**) Atomic geometries of Janus MSX (M = Mo,

W) [39]; (**g**) Magnitudes of the binding energies of Na_2Sn with MoSTe, DME, and DOL calculated by DFT-D3 method. For comparison the Eb values of Na_2Sn with MoSTe monolayer without van der Waals corrections are also given [39]; (**h**) Energy barriers of Na_2S decomposition ($Na_2S \rightarrow NaS^+ Na^+$) on MoSTe monolayer. The corresponding diffusion path on MoSTe monolayer is shown by the inset [39].

2.3 Construction of Heterogeneous Structures

The incorporation of heteroelements (e.g., Ce, N) for fabricating composite heterostructures realizes multifunctional synergistic effects, including physical confinement, chemical adsorption, catalytic conversion, and interface regulation, thereby further enhancing the cathode performance.

Liu et al. [38] fabricated a CeO_2-QDs/HPC bifunctional host via CeO2 quantum dot modification of 3D hierarchical porous carbon (HPC) (CeO_2-QDs). This host ACTS as both a supporting matrix for the Te cathode and as a dendrite inhibitor for the sodium anode. Within the Te/CeO_2-QDs/HPC cathode, CeO_2-QDs provide abundant catalytic active sites, facilitating the rapid interconversion between Te and Na_xTe, while the porous structure of HPC alleviates volume expansion. The full cell assembled with this cathode and a Na/CeO_2-QDs/HPC anode, retains a capacity of 260 $mAh{\cdot}g^{-1}$ and achieves an energy density of 192 $Wh{\cdot}kg^{-1}$ after 1000 cycles at a rate of 10 C. Pyridinic N, pyrrolic N, and quaternary N within the nitrogen-doped carbon support enhance the adsorption capacity for polytellurides via charge transfer mechanisms, concurrently enhancing electronic conductivity [44]. This allows the NPCS/Te cathode to maintain stable Na-storage performance even at a high discharge rate of 10 C.

3 Applications of Tellurium and Tellurides in the Regulation and Protection of Anode Interfaces

Tellurium (Te) and its tellurides demonstrate distinctive advantages in the regulation and protection of anode interfaces, owing to their high ionic conductivity, favorable sodium affinity, and robust structural stability. Through mechanisms such as the formation of artificial solid-electrolyte-interphase (SEI) layers, optimization of sodium deposition patterns, and suppression of dendrite growth, the electrochemical performance of sodium metal anodes is markedly improved (Table 2).

Table 2: Performance comparison of tellurium and telluride in anode interface control and protection.

System Type	Cathode Material	Cycling	Rate	Citation
Na-Metal Battery	Na@Na_2Te	1 $mA{\cdot}cm^{-2}$, 700 h; stable plating/stripping	20 C/3000 cycles, 93% retention	[36]
Na-Metal Battery	High-entropy telluride@CC (HET@CC)	0.5 $mA{\cdot}cm^{-2}$, 2000 h; CE > 99.5%	0.25 $mA{\cdot}cm^{-2}$, 600 h quasi-solid-state	[35]
Na-Metal Battery	Na-Sn-Sn-Na_2Te (NST)	1 $mA{\cdot}cm^{-2}$, 1390 h; stable cycling	5 C/1000 cycles, 88% retention	[45]
Na-Metal Battery	Na-Sb-Te intermetallic (NST-Na)	1 $mA{\cdot}cm^{-2}$, 1000 h; 100% DOD, CE = 99.4%	anode-free, 0.23% decay per cycle	[46]

3.1 Optimization of Sodium Ion Transport Kinetics

Tellurides (such as Na_2Te, NST composite layer) exhibit low sodium ion diffusion energy barriers and high ionic conductivity, which can accelerate the transport of sodium ions at the interface and mitigate dendrite growth caused by ion concentration gradients.

During the adsorption stage, electronegative Te atoms on the telluride surface engage in robust chemical interactions with sodium ions, leading to a notable reduction in the adsorption energy barrier. The adsorption energy of sodium ions at the hollow sites on the (001) crystal plane of Na_2Te attains a

value of −3.371 eV (Fig. 4a), significantly lower than the −0.951 eV observed on the bare sodium surface. This disparity renders sodium ions more likely to adsorb onto the telluride surface [36]. The sodium ion adsorption energies of the alloying products Na_3Sb and Na_3Bi in high-entropy tellurides (HETs) are −0.6388 eV (Fig. 4b) and −0.5396 eV, respectively, further strengthening the thermodynamic adsorption advantage [35]. The crystal structure of tellurides provides efficient ion transport channels. Na_2Te adopts an inverse fluorite structure (Fig. 4c), with an ion diffusion barrier along the [100] direction of only 0.28 eV. At 300 K, its diffusion coefficient reaches 3.7×10^{-10} cm^2/s, which can rapidly eliminate the sodium ion concentration gradient at the interface [36]. The heterointerface formed between Na_2Te and Na-Sn alloy in the NST composite layer (Fig. 4d) reduces the activation energy for sodium ion diffusion to 40.9 kJ/mol, which is superior to the 66.5 kJ/mol of bare sodium [45]. Thermodynamic driving forces and physical constraints synergistically promote compact sodium deposition. The three-dimensional interconnected structure of the NST framework guides the "filling" growth of sodium (Fig. 4e), forming a non-porous, compact layer [46]. The high-entropy effect of HET@CC transforms sodium deposition from "island growth" to "planar spreading" (Fig. 4f), resulting in a uniform thickness of the deposition layer [36].

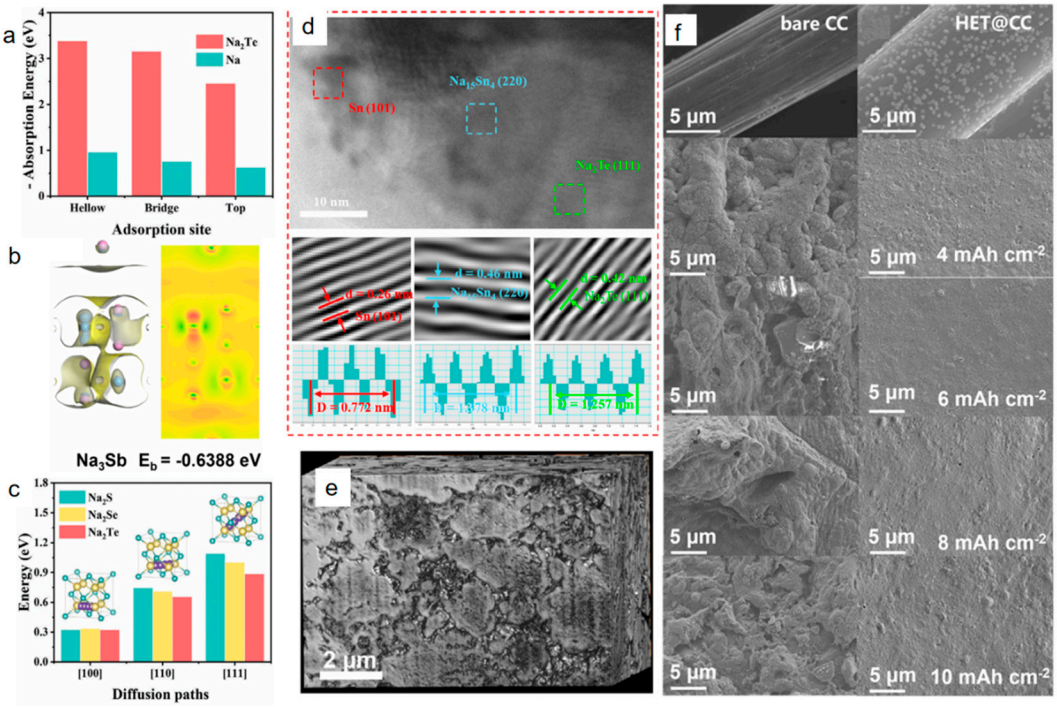

Figure 4: (**a**) A summary of adsorption energies of Na^+ on the Na_2X (X = S, Se, Te) [36]; (**b**) Differential charge density of Na^+ adsorption on Na_3Sb [35]; (**c**) A summary of diffusion energy barriers of Na^+ in the Na_2X (X = S, Se, Te). The inset is the schematic diagram of the Na^+ diffusion paths along the [100], [110], and [111] directions [36]; (**d**) high-resolution cryo-TEM image and the corresponding inverse fast Fourier transform images of the artificial NST interlayer [45]; (**e**) FIB-SEM tomography of NST, highlighting its interconnected 3D structure [46]; (**f**) FESEM images of bare CC and HET@CC with various sodium plating capacities [35].

3.2 SEI Layer Component-Structure Synergistic Optimization Mechanism

Telluride participates in the formation of the SEI layer, constructing a multifunctional interface layer with "high stability, high conductivity, and high mechanical strength", breaking the performance bottleneck of traditional SEI layers.

The NST artificial SEI is *in-situ* formed via the reaction between SnTe and Na metal (Fig. 5a), yielding a uniform interlayer composed of Na_2Te, Na–Sn alloy and Sn. In terms of component optimization, telluride guides the formation of an inorganic-phase-dominated composite structure with an SEI layer. The SEI derived from the NST composite layer is rich in inorganic components such as Na_2Te and NaF. Among them, the ionic conductivity of Na_2Te (10^{-4} S cm^{-1}) is much higher than that of the organic phase, while NaF provides high mechanical strength [45]. In the SEI layer of the Na@Na_2Te anode, Na_2Te forms an interpenetrating network with NaF and Na_2CO_3, inhibiting the continuous decomposition of the electrolyte [35]. Cryo-TEM observation confirms a bilayer SEI structure with an inner nanocrystalline region rich in Na_2Te, NaTe and NaF, verifying the inorganic-dominated feature (Fig. 5b). The SEI layer derived from HET@CC is rich in NaF, featuring both a high Young's modulus and a low sodium diffusion barrier [36]. In terms of structural optimization, telluride regulation results in a uniform and dense microstructure of the SEI layer. The NST composite layer guides the SEI layer thickness to be controlled between 20 and 50 nm, with no obvious pores [45]. Due to the improved uniformity of sodium deposition, HET@CC features a "thin and dense" solid electrolyte interphase (SEI) layer, resulting in a charge transfer resistance of only 6 Ω [36]. The 3D interconnected NST skeleton, which offers homogeneous sodiophilic sites and stabilizes SEI growth (Fig. 5c).

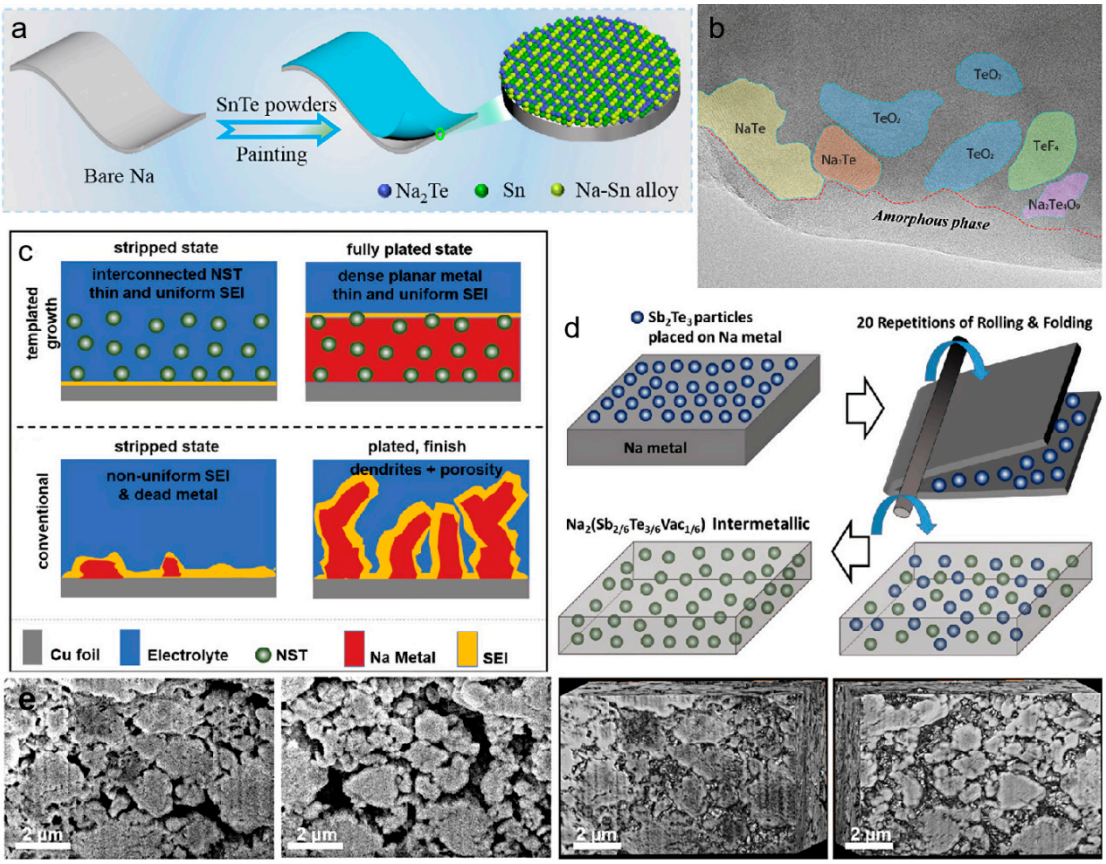

Figure 5: (**a**) Schematic illustration of the fabrication procedure of the Na/NST [45]; (**b**) Cryo-TEM image and phase compositions mapping of SEI of Na@Na2Te [36]; (**c**) Illustration of NST enhancement effect on the plating and stripping behavior [46]; (**d**) Illustration for the fabrication process of sodium-antimony-telluride-Na metallurgical composite, termed NST-Na [46]; (**e**) FIB cross-sectional SEM images and FIB-SEM tomography of NST, highlighting its interconnected 3D structure, showing the front views and the back views, respectively [46].

Fig. 5C reveals the 3D interconnected NST skeleton, which offers homogeneous sodiophilic sites and stabilizes SEI growth. In terms of performance optimization, the dynamic stability of the SEI layer is significantly enhanced. Na_2Te exhibits strong chemical inertness and is resistant to decomposition during cycling [45]. The SEI component of the NST composite layer remains stable even after 1000 cycles. The SEI layer derived from high-entropy tellurides can buffer volume changes through its own deformation, preventing repeated cracking and reconstruction [36]. The Na_2Te/NST-modified SEI is thin and compact, whereas the pristine SEI on bare Na is thick, porous and accompanied by serious dendrite growth (Fig. 5c).

In addition to the above two aspects, telluride can also inhibit dendrite growth and propagation through the dual effects of "physical mechanical constraints + uniform charge distribution" (Fig. 5d) [46]. The 3D interconnected NST framework guides the "filling" growth of sodium, forming a non-porous, compact layer [46]. FIB cross-sectional SEM images and FIB-SEM tomography of NST further highlight its interconnected 3D structure (Fig. 5e).

4 Tellurium-Based Performance Optimization Modification Strategy

Using tellurium or tellurium compounds as core modifiers, strategies such as eutectic acceleration, defect engineering, and multicomponent synergy overcome the interfacial matching bottleneck among cathode–anode–electrolyte in sodium metal batteries, simultaneously enhancing reaction kinetics, cycling stability, rate capability, and energy density of full cells, enabling systematic cross-component optimization. To strengthen mechanistic analysis, adsorption energies, diffusion barriers, and catalytic effects scattered in the text are consolidated into a compact comparison table (Table 3).

Table 3: Summary of Adsorption Energy, Na^+ Diffusion Barrier, Catalytic Performance, and References.

Modification Strategy	Typical Material System	Adsorption Energy (eV)	Na^+ Diffusion Barrier (eV)	Key Performance	Citation
Eutectic acceleration	$Te_{0.04}S_{0.96}$@pPAN	—	0.42	Capacity decay: 0.015% per cycle	[47]
Defect engineering	Te vacancy + F-doped $CoTe_{2-x}F$	Na–pTe/Te_8: −2.93	0.12	2000 cycles at 1 $A{\cdot}g^{-1}$, decay 0.016%	[48]
Alloying	Sb_2Te_3@CC	Na^+@Na_3Sb: −0.241	—	1600 h, overpotential 30.5 mV	[29]
Solid-state electrolyte	$Na_2Zn_2TeO_6$	—	0.25	D: 8.5×10^{-8} $cm^2{\cdot}s^{-1}$	[49]
Te–S heterocatalysis	Janus MoSTe/$MoTe_2$	Na_2S_n: −1.18 ~ −2.48	0.10 ~ 0.11	Enhanced polysulfide conversion	[50]

4.1 Eutectic Acceleration Mechanism and Application

The eutectic acceleration mechanism utilizes Te and chalcogenides (S, sulfurized polyacrylonitrile) to form a molecular-level dispersed system, enhancing battery performance by regulating reaction kinetics and interfacial characteristics. Te, as an eutectic accelerator, can improve electronic conductivity, reduce the migration energy barrier of Na^+, accelerate the redox conversion of polysulfides, and simultaneously inhibit the agglomeration and dissolution of active materials [47].

The $Te_{0.04}S_{0.96}$@pPAN composite material designed by Li et al. [42] exhibits a discharge specific capacity of 629 $mAh{\cdot}g^{-1}$ in carbonate electrolyte and 601 $mAh{\cdot}g^{-1}$ in ether electrolyte at 6 $A{\cdot}g^{-1}$ (Fig. 6a). UV-visible spectroscopy and shuttle current tests confirm that Te doping significantly reduces the content of soluble polysulfides in the electrolyte (Fig. 6b). After 600 cycles at 0.5 $A{\cdot}g^{-1}$, the decay rate is only 0.015% (Fig. 6c). This mechanism exhibits universality in room-temperature sodium-sulfur batteries, broadening the electrolyte compatibility window and providing a feasible path for practical application.

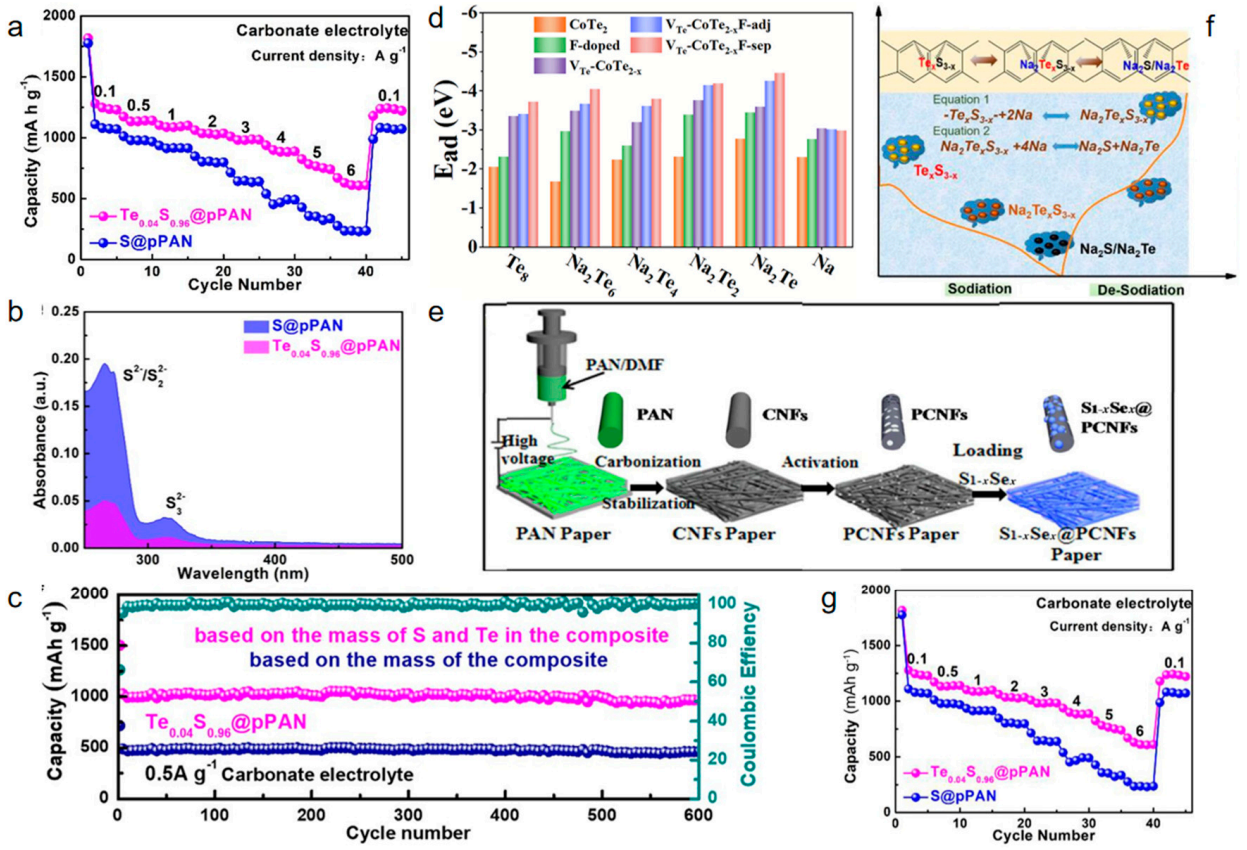

Figure 6: (**a**) The electrochemical performance of $Te_{0.04}S_{0.96}$@pPAN and S@pPAN in carbonate and ether electrolytes; (**b**) The long cycle performance of $Te_{0.04}S_{0.96}$@pPAN-Na cells at 0.5 $A{\cdot}g^{-1}$ in carbonate electrolyte. (**c**) The UV-visible spectrum of $Te_{0.04}S_{0.96}$@pPAN and S@pPAN cathodes in ether electrolyte; (**d**) Adsorption energies of Na-pTe/Te_8-$CoTe_{2-x}$ molecules and Na atoms on different surfaces; (**e**) Schematic of the synthesis of a $S_{1-x}Se_x$@PCNFs electrode; (**f**) Proposed reaction pathway of a $Te_{0.04}S_{0.96}$@pPAN cathode; (**g**) Rate performance comparison of $Te_{0.04}S_{0.96}$@pPAN and S@pPAN in carbonate electrolytes.

4.2 Defective Engineering and Doping Modification

Defect engineering and doping modification optimize the intrinsic properties of materials by regulating the crystal structure and electronic state distribution of Te-based materials, encompassing two approaches: single defect control and composite modification.

Single defect regulation, represented by the introduction of Te vacancies (Te), breaks the integrity of the crystal lattice to form active sites, enhances the adsorption and catalytic conversion of poly-telluride intermediates, and reduces the reaction energy barrier [48]. In the composite modification strategy, the synergistic effect of F doping and Te vacancies (Te-$CoTe_{2-x}F$) constructs dual active sites. The Te vacancies form Te-philic sites, while the F atoms form Na-philic sites, achieving simultaneous strong adsorption of the Na-pTe intermediate (Fig. 6d). This synergistic effect enhances the adsorption energy by 23.19%–29.28%, while maintaining the metallic conductivity and reducing the Na^+ diffusion energy barrier.

In addition, Ga and Ca co-doping in $Na_2Zn_2TeO_6$ can optimize the ion transport channels, achieving a maximum ionic conductivity of 0.75×10^{-3} S/cm at room temperature [49].

4.3 Multi-Component Collaborative Optimization

Multi-component synergistic optimization constructs an integrated "structure-function" system through functional complementarity, encompassing three pathways: Janus structure design, support-telluride-catalyst synergy, and cross-scale multilevel regulation.

In the synergistic system of carrier-telluride-catalyst, carbon carrier (carbon cloth, porous carbon nanofibers, 3D graphene, etc.) plays multiple roles (Fig. 6e). Not only providing a specific surface area and developed porous structure to achieve uniform dispersion and physical confinement of Te-based active components, but also constructing efficient electron transport channels, reducing charge transfer resistance, and alleviating volume expansion during cycling (Fig. 6f) [42]. Te-based compounds (such as Sb_2Te_3, $Te_{0.04}S_{0.96}$, etc.) serve as the core active components. Their high conductivity and unique electronic structure endow the system with excellent sodium-storage activity. At the same time, they can act as catalytic sites to accelerate the conversion of polysulfides/polytellurides [50]. In Sb_2Te_3@CC, the carbon cloth constructs a 3D framework, and Sb_2Te_3 generates Na_3Sb (nucleation sites) and Na_2Te (stabilizing SEI film), resulting in a symmetric battery with an overpotential of only 30.5 mV after 1600 h of cycling [29]. Cross-scale regulation achieves multi-level optimization from macrostructure (3D hierarchical structure), microdefects (vacancies/doping) to electronic structure (charge distribution). For example, VTe-$CoTe_{2-x}F$ and $Te_{0.04}S_{0.96}$@pPAN both achieve synergistic performance enhancement through this strategy (Fig. 6g) [48,51].

5 Summary and Challenges

Tellurium and tellurides, with their excellent electrochemical properties, have become key functional materials for optimizing the performance of sodium metal batteries. Their application has achieved multi-functional regulation of the battery's cathode, anode, and the full-cell system.

At the cathode, the hybridization of tellurium and tellurides with carbon-based materials can through physical confinement uppress the shuttle effect and volume expansion of polytellurides via physical confinement effects, consequently enhancing electron transport efficiency. When alloyed with chalcogens like sulfur and selenium, or with transition metals, chemical interactions can be harnessed to enhance the adsorption of reaction intermediates and regulate electrochemical kinetics, thereby fundamentally addressing critical issues such as poor conductivity and sluggish reaction kinetics in the positive electrode. At the anode, the utilization of tellurium and tellurides to construct an artificial solid electrolyte interphase (SEI) layer, protective coating, or three-dimensional host framework effectively alleviates issues such as dendrite growth, interfacial instability, and electrolyte decomposition in sodium metal anodes, thereby ensuring the long-term cycling safety and reversibility of the anode. In the realm of performance optimization and modification, tellurium and its tellurides serve as pivotal modifiers. By employing strategies such as eutectic acceleration, defect engineering, and multicomponent synergism, they have successfully addressed the bottleneck associated with the matching of interface matching bottleneck among cathode, anode, and electrolyte. This advancement has led to synergistic enhancements in full-cell reaction kinetics, cycling stability, rate capability, and energy density, thereby providing a systematic optimization scheme for the performance upgrading of sodium metal batteries. Overall, the introduction of tellurium and tellurides has breaks through the limitations of single-factor regulation in sodium metal batteries, achieving synchronous enhancement in the performance of both the positive and negative electrodes. This has become an important research direction for promoting the practical development of sodium metal batteries.

Despite the remarkable progress achieved, several critical challenges must be addressed for practical deployment. First, the natural scarcity and high extraction cost of tellurium restrict large-scale commercialization,

and the rational design of low-tellurium, high-efficiency composite systems and tellurium recycling technologies are urgently needed. Second, a quantitative trade-off exists between volumetric and gravimetric energy density: although sulfur delivers a much higher theoretical gravimetric capacity (1672 $mAh{\cdot}g^{-1}$), its ultralow density (2.07 $g{\cdot}cm^{-3}$), insulating nature, and severe shuttle effect lead to poor practical volumetric energy density and rapid capacity fading. In contrast, tellurium has a moderate theoretical gravimetric capacity (420 $mAh{\cdot}g^{-1}$) but a much higher density (6.2 $g{\cdot}cm^{-3}$) and metal-level electronic conductivity, enabling superior volumetric capacity, long-cycle stability, and high-rate capability in real devices. For compact energy storage systems requiring high volumetric performance and safety, tellurium-based materials are more competitive than sulfur-based systems. Meanwhile, the structural durability of telluride-based electrodes under long-term high-rate cycling remains insufficient, and severe volume expansion may still cause structural collapse and active-material loss. In addition, the detailed reaction pathways and intermediate evolution mechanisms of tellurium-based electrodes are still not fully elucidated, limiting the precise material design.

Future research should focus on four aspects to promote industrial application. First, develop low-tellurium or tellurium–sulfur/selenium composite systems to reduce raw-material cost and dependence on tellurium resources, while exploring efficient tellurium recovery processes. Second, combine *in-situ* characterization and theoretical calculations to clarify the conversion mechanism of tellurium-based materials, the shuttle behavior of polytellurides, and interface evolution rules, providing a solid basis for precise structural design. Third, optimize electrode structures through nanocrystallization, defect engineering, and heterostructure construction to improve structural stability and relieve volume expansion. Fourth, develop low-cost, scalable preparation processes and explore full-cell integration design to realize synergistic optimization of cathode, anode, and electrolyte, thereby building high-performance, low-cost, and high-safety sodium metal batteries based on tellurium and tellurides.

Acknowledgement: The authors thank the Natural Science Foundation of Henan, Zhengzhou Foundation for Basic Research and Postgraduate Education Reform and Quality Improvement Project of Henan Province to provide project fund support. The authors further thank all individuals who contributed directly or indirectly to this work.

Funding Statement: This research was funded partly by Natural Science Foundation of Henan (252300423714); the Zhengzhou Foundation for Basic Research (grant numbers ZZSZX202414 and ZZSZX202412) and the Postgraduate Education Reform and Quality Improvement Project of Henan Province (YJS2025GZZ63).

Author Contributions: Study conception and design: Fei Wang, JinPing Zhang; data collection: Shan Yuan, Yuxin Jiang, Kaibo Gu, Chenhao Qiao, Yutong Bai, Jie Yu; analysis and interpretation of results: Shan Yuan; draft manuscript preparation: Shan Yuan. review and editing, Fei Wang, JinPing Zhang, Quan Chen, Dedi Han. All authors reviewed and approved the final version of the manuscript.

Availability of Data and Materials: The authors confirm that the data supporting the findings of this study are available from the corresponding authors upon reasonable request.

Ethics Approval: Not applicable.

Conflicts of Interest: The authors declare no conflicts of interest.

References

1. Qiu S, Zhu H, Wu Q, Cheng S, Xie J. Failure mechanisms and current collector design for sodium metal anodes: From thermodynamic-kinetic coupling to structural-functional optimization. Energy Storage Mater. 2026;85:2405–8297. [CrossRef].

2. Ge J, Ma C, Wan Y, Tang G, Dai H, Sun S, et al. Electrocatalysis of Fe-N-C Bonds Driving Reliable Interphase and Fast Kinetics for Phosphorus Anode in Sodium-Ion Batteries. Adv Funct Mater. 2023;33(47):2305803. [CrossRef].
3. Walle KZ, Pandeeswari J, Jenisha G, Kotobuki M. Li-Na-based hybrid battery. Funct Mater Lett. 2023;16(02):2340011. [CrossRef].
4. Pandurangan I, Kannadasan M, Balakrishnan M. Understanding structural and electrochemical properties of metal-doped NASICON-type solid polymer electrolytes for all-solid-state sodium-metal batteries. Next Energy. 2026;11:100558. [CrossRef].
5. Cao RG, Mishra K, Li XL, Qian JF, Engelhard MH, Bowden ME, et al. Enabling room temperature sodium metal batteries. Nano Energy. 2016;30:825–30. [CrossRef].
6. Zhou S, Chen X, Zhang X, Kuang W, Jiao C, Xu X, et al. Recent progress on organic liquid electrolyte for high-temperature sodium batteries. Adv Funct Mater. 2025;35(29):169980. [CrossRef].
7. Sun B, Li P, Zhang JQ, Wang D, Munroe P, Wang CY, et al. Dendrite-free sodium-metal anodes for high-energy sodium-metal batteries. Adv Mater. 2018;30(29):1801334. [CrossRef].
8. Gao W, Xi G, Cao J, Jia A, Wang C, Ullah S, et al. Artificial interphase layers on sodium metal anodes: Preparation strategies, design principles, and future outlook. J Mater Chem A. 2026;14:13286–307. [CrossRef].
9. Teli AM, Beknalkar SA, Satale VV, Yewale MA, Amate RU, Morankar PJ, et al. Innovations in metal telluride composite materials towards enhancing supercapacitor energy storage. J Alloys Compd. 2024;1005:175950. [CrossRef].
10. Manikandan M, Subramani K, Sathish M, Dhanuskodi S. Hydrothermal synthesis of cobalt telluride nanorods for a high performance hybrid asymmetric supercapacitor. RSC Adv. 2020;10(23):13632–41. [CrossRef].
11. Zhang S, Yang D, Zhang M, Liu Y, Xu T, Yang J, et al. Synthesis of novel bimetallic nickel cobalt telluride nanotubes on nickel foam for high-performance hybrid supercapacitors. Inorg Chem Front. 2019;7(2):477–86. [CrossRef].
12. Patil GP, Jadhav CD, Lyssenko S, Minnes R. Hydrothermally synthesized copper telluride nanoparticles: First approach to flexible solid-state symmetric supercapacitor. Chem Eng J. 2024;498:155284. [CrossRef].
13. Wu Q, Wu YK, Yan H, Zhong W, Qin MS, Zhu HL, et al. A cross-linked nanoflower network and Se-doping enabling sulfur-rich SPAN towards lithium-sulfur batteries beyond 600 W h kg^{-1}. Energy Environ Sci. 2025;18(10):4905–15. [CrossRef].
14. Xue Z, Yang S, Zhang S, Xing L, Lee S, Park HS, et al. Review on the application of nanocarbon materials for lithium and sodium metal batteries. Energy Mater Adv. 2025;6(28):0415. [CrossRef].
15. Tian R, Xie M, Shi Z. Advanced anodes and compatible electrolyte strategies for next-generation Li/Na batteries. Chem A Eur J. 2026. [CrossRef].
16. Kwon DS, Gong SH, Yun S, Jeong D, Je J, Kim HJ, et al. Regulating Na electrodeposition by sodiophilic grafting onto porosity-gradient gel polymer electrolytes for dendrite-free sodium metal batteries. ACS Appl Mater Interfaces. 2022;14(42):47650–8. [CrossRef].
17. Lin J, Huang P, Wu Y, Yan K, Liang C, Zhang C, et al. Heterogeneous cations enable crystallographic regulation of na deposition toward dendrite-free sodium metal batteries. ACS Energy Lett. 2026;11(3):2789–97. [CrossRef].
18. Shiraz MHA, Zhao P, Liu J. High-performance sodium-selenium batteries enabled by microporous carbon/selenium cathode and fluoroethylene carbonate electrolyte additive. J Power Sources. 2020;453:227855. [CrossRef].
19. Lee S, Lee J, Kim J, Agostini M, Xiong S, Matic A, et al. Recent developments and future challenges in designing rechargeable potassium-sulfur and potassium-selenium batteries. Energies. 2020;13(11):2791. [CrossRef].
20. Wang R, Wang DG, Dong Y, Xie B, Wu XY, Wu QH, et al. Recent progress of advanced carbon-based cathode in sodium-selenium batteries. J Alloys Compd. 2023;952:169980. [CrossRef].
21. Ali M, Chishti AN, Ali M, Iqbal S, Aman S, Mahmood A, et al. Recent development in sodium metal batteries: Challenges, progress, and perspective. Mater Today. 2025;88:730–51. [CrossRef].
22. Chang W, Su X, Wang H, Tao Z, Tao H, Ma H, et al. A functional Na_xSn/NaBr interlayer for solid-state sodium metal batteries. Chem Eng J. 2026;530:173413. [CrossRef].
23. Wu Q, Zhang W, Qin MS, Zhong W, Yan H, Zhu HL, et al. Tellurium doped sulfurized polyacrylonitrile nanoflower for high-energy-density, long-lifespan sodium-sulfur batteries. Nano Energy. 2024;129:110049. [CrossRef].

24. Ruiz R, Pérez-Vicente C, Alcántara R. Metallic particles in sodium battery anodes: A review. Micromachines. 2025;16(12):1391. [CrossRef].
25. Song J, Jeong G, Lee AJ, Park JH, Kim H, Kim YJ. Dendrite-free polygonal sodium deposition with excellent interfacial stability in a $NaAlCl_4$-$2SO_2$ Inorganic Electrolyte. ACS Appl Mater Interfaces. 2015;7(49):27206–14. [CrossRef].
26. Xiao Y, Lee SH, Sun YK. The application of metal sulfides in sodium ion batteries. Adv Energy Mater. 2016;7(3):1601329. [CrossRef].
27. Fan H, Dai Y, Xue X, Zheng R, Wang Y, Arandiyan H, et al. Modification, application and expansion of electrode materials based on cobalt telluride. J Energy Chem. 2024;97:710–37. [CrossRef].
28. Dai YY, Xu CM, Liu XH, He XX, Yang Z, Lai WH, et al. Manipulating metal-sulfur interactions for achieving high-performance S cathodes for room temperature Li/Na-sulfur batteries. Carbon Energy. 2021;3(2):253–70. [CrossRef].
29. Chen B, Zhao Y, Yuan B, Zhu Y, Chong S. Antimony telluride as bifunctional host material for dendrite-free sodium metal batteries. Nano Lett. 2025;25(12):4869–77. [CrossRef].
30. Zhu J, Zou JL, Cheng H, Gu YY, Lu ZG. High energy batteries based on sulfur cathode. Green Energy Environ. 2019;4(4):345–59. [CrossRef].
31. Feng JN, Yu SX, Shi C, Tang X, Zhao XX, Chen SQ, et al. Advanced cathode designs for high-energy lithium/sodium-selenium battery. Adv Funct Mater. 2025;35(24):2422013. [CrossRef].
32. Zhang Y, Manaig D, Freschi DJ, Liu J. Materials design and fundamental understanding of tellurium-based electrochemistry for rechargeable batteries. Energy Storage Mater. 2021;40:166–88. [CrossRef].
33. Sung G-K, Nam K-H, Choi J-H, Park C-M. Germanium telluride: Layered high-performance anode for sodium-ion batteries. Electrochimica Acta. 2020;331:135393. [CrossRef].
34. Ahmed S, Ghani A, Mehmood R, Ali A, Hussain N, Khaliq A, et al. Ultra-stable topological telluride monolayers for next-generation battery anodes and sulfur hosts. Adv Sci. 2026;13(4):e15841. [CrossRef].
35. Zhao Y, Wang Z, Chen Y, Qiao S, Wu Y, Liu HK, et al. High-entropy telluride as multifunctional host material with synergistic conversion-alloying chemistry of dendrite-free sodium metal anode for quasi-solid-state batteries. Nano Lett. 2026;26(9):3080–9. [CrossRef].
36. Yang H, He F, Li M, Huang F, Chen Z, Shi P, et al. Design principles of sodium/potassium protection layer for high-power high-energy sodium/potassium-metal batteries in carbonate electrolytes: a case study of Na_2Te/K_2Te. Adv Mater. 2021;33(48):2106353. [CrossRef].
37. Han MS, Zhou ZH, Li Y, Chen QG, Chen MH. Highly conductive tellurium and telluride in energy storage. Chem Electrochem. 2021;8(23):4412–26. [CrossRef].
38. Liu Y, Li J, Hu X, Yuan J, Zhong G, Zhang L, et al. CeO_2 quantum-dots engineering 3D carbon architectures toward dendrite-free Na anode and reversible Te cathode for high-performance Na-Te batteries. Infomat. 2022;4(10):e12343. [CrossRef].
39. Wang H, Tong Z, Yang R, Huang Z, Shen D, Jiao T, et al. Electrochemically stable sodium metal-tellurium/carbon nanorods batteries. Adv Energy Mater. 2019;9(48):190346. [CrossRef].
40. Koketsu T, Wu C, Huang Y, Strasser P. A high-performance Te@CMK-3 composite negative electrode for Na rechargeable batteries. J Appl Electrochem. 2018;48(11):1265–71. [CrossRef].
41. Sun F, Zhang B, Tang H, Yue Z, Li X, Yin C, et al. Heteroatomic $TexS_{1-x}$ molecule/C nanocomposites as stable cathode materials in carbonate-based electrolytes for lithium-chalcogen batteries. J Mater Chem A. 2018;6(21):10104–10. [CrossRef].
42. Gao W, Song B, Zhang Q, He J, Wu Y. 3D flower-like nanospheres constructed by transition metal telluride nanosheets as sulfur immobilizers for high-performance room-temperature Na-S batteries. Small. 2024;20(23):2310225. [CrossRef].
43. Kaewmaraya T, Thatsami N, Tangpakonsab P, Klinkla R, Kotmool K, Hussian T. Revealing the binding mechanism of redox intermediates in sodium–sulfur batteries by two-dimensional Janus monolayers. J Power Sources. 2023;585:233639. [CrossRef].
44. Li Y, Zhan Y, Xu Q, Hu L, Shen B, Liu H, et al. Nitrogen-doped carbon as a host for tellurium for high-rate Li-Te and Na-Te batteries. Chemsuschem. 2019;12(6):1196–202. [CrossRef].

45. Xia X, Chen K, Xu S, Yao Y, Liu L, Xu C, et al. Robust artificial interlayer with high ionic conductivity and mechanical strength toward long-life Na-metal batteries. Small Sci. 2023;3(7):2300038. [CrossRef].
46. Wang Y, Dong H, Katyal N, Hao H, Liu P, Celio H, et al. A sodium-antimony-telluride intermetallic allows sodium-metal cycling at 100% depth of discharge and as an anode-free metal battery. Adv Mater. 2022;34(1):2106005. [CrossRef].
47. Li S, Zeng Z, Yang J, Han Z, Hu W, Wang L, et al. High performance room temperature sodium-sulfur battery by eutectic acceleration in tellurium-doped sulfurized polyacrylonitrile. ACS Appl Energy Mater. 2019;2(4):2956–64. [CrossRef].
48. Huang J, Li W, Guo Y, Tong L, Lin H, Cheng Y, et al. Synergistic vacancy and fluorine doping in metallic 1T-$CoTe_2$ for high-performance sodium-tellurium battery cathodes. Appl Surf Sci. 2026;727:165961. [CrossRef].
49. Li X, Bianchini F, Wind J, Vajeeston P, Wragg D, Fjellvag H. P2 type layered solid-state electrolyte $Na_2Zn_2TeO_6$: crystal structure and stacking faults. J Electrochem Soc. 2019;166(15):A3830. [CrossRef].
50. Wang Y-H, Li X-T, Wang W-P, Yan H-J, Xin S, Guo Y-G. Chalcogen cathode and its conversion electrochemistry in rechargeable Li/Na batteries. Sci China Chem. 2020;63(10):1402–15. [CrossRef].
51. Li S, Zhang W, Zeng Z, Cheng S, Xie J. Selenium or tellurium as eutectic accelerators for high-performance lithium/sodium-sulfur batteries. Electrochem Energy Rev. 2020;3(3):613–42. [CrossRef].